Dynamical phase transition of a periodically driven DNA

Garima Mishra,[1] Poulomi Sadhukhan,[2] Somendra M. Bhattacharjee,[2] and Sanjay Kumar[1]
[1]*Department of Physics, Banaras Hindu University, Varanasi 221 005, India*
[2]*Institute of Physics, Bhubaneswar 751 005, India*
(Received 26 April 2012; published 25 February 2013)

Replication and transcription are two important processes in living systems. To execute such processes, various proteins work far away from equilibrium in a staggered way. Motivated by this, aspects of hysteresis during unzipping of DNA under a periodic drive are studied. A steady-state phase diagram of a driven DNA is proposed which is experimentally verifiable. As a two-state system, we also compare the results of DNA with that of an Ising magnet under an asymmetrical variation of the magnetic field.

DOI: 10.1103/PhysRevE.87.022718 PACS number(s): 87.15.−v, 05.70.Ln, 75.40.Gb, 87.10.Tf

I. INTRODUCTION

The semiconservative replication of DNA requires a complete separation of the two strands, which occurs concomitantly with the production of new strands. Even transcription needs a partial separation of the two strands of DNA to read the genetic code of the base sequence [1]. The traditional view of a temperature- or pH-induced melting is being superseded by a more mechanical procedure of force- or torque-induced unzipping [2–5]. This paradigm shift is because of the lack of extreme temperatures or the environment required in general for the melting (the melting temperature is around 70–100 °C) and the recent establishment of the unzipping as a genuine phase transition [2]. A double-stranded (ds) DNA remains in the bound doublet state below its melting temperature even when pulled by a force at one end until and unless the force exceeds a critical force, $g = g_c(T)$, above which it opens into two single-stranded (ss) DNA. Many aspects of this transition have been studied since then, both theoretically [6–15] and experimentally [4,16,17], mostly in equilibrium, though puzzles remain [18,19].

In vivo, DNA is opened by helicases, which are motors that move along the DNA [1]. Both the motion and the opening processes require a constant supply of energy. A few examples are DNA-B, a ringlike hexameric helicase that pushes through the DNA like a wedge [20]; PcrA, which goes through cycles of pulling the ds part of the DNA and then moving on the ss part [21]; and viral RNA helicase nucleoside triphosphate phosphohydrolase-II (NPH-II), which hops cyclically from the ds to the ss part of the DNA and back [22]. Such cycles of action and rest, with the periodic adenosine triphosphate (ATP) consumption, indicates an exertion of a periodic force on the DNA.

It suffices to describe the equilibrium unzipping transition by the two thermodynamic conjugate variables, force g and separation x of the pulled base pair (Fig. 1). In thermal equilibrium, a quasistatic change of the force from zero to a maximum g_m and then back to zero, keeping other intensive quantities fixed, would result in retracing the thermodynamic path, ending at the initial state; history plays no role because of ergodicity. In contrast, under a periodic force, the mismatch between the relaxation time and the external time scale for change of force would restrict the DNA to explore a smaller region of the phase space, creating a difference in the response to an increasing or a decreasing force. Near a phase transition, where the typical time scales of dynamics become large, the difference between the forward and the backward branches becomes prominent. This is hysteresis of DNA unzipping [23]. More recently Kapri [24] showed how the work theorem can be used *via* a multihistogram method to extract the equilibrium isotherm from the hysteresis curves. The nature of hysteresis and its dependence on the applied field and frequency are well studied in the context of magnetic and structural systems [25,26], though it is the time-averaged loop that has received the attention. With the advent of single-molecule experiments on short DNA chains (oligomers), it might be possible to probe the time-resolved loops, not just averages. Motivated by the biological relevance and the experimental feasibility, we explore the behavior of DNA under a periodic force, to be called a *periodically driven DNA*. Our results show that without changing the physiological conditions (e.g., the temperature or pH of the solvent), a DNA chain may be brought from the unzipped state to the zipped state and *vice versa* by varying the frequency (ν) alone. By using a probabilistic description of the time variation of the DNA response, we propose a force-frequency (g-ν) phase diagram for the driven DNA.

A similar dynamic symmetry breaking transition is known to occur in magnets where the nature of the hysteresis loop changes [26]. Because of the two stable phases, the unzipping transition has often been described by a two-state Landau-type free energy functional [5,12,27]. As a two-phase system, we make use of the magnetic Ising model to corroborate the behavior of DNA, both undergoing a first-order transition and showing hysteresis. We establish that the observed features and the phase diagram are robust and generic, and not tied to any particular DNA model.

It was recently shown that the DNA hairpin (Fig. 1) of 32 beads (stem 10 base pairs and a loop of 12 bases) captures the essential properties of a long DNA chain with implicit bubbles [23]. The force-temperature diagram of the DNA hairpin is found to be qualitatively similar to that of the DNA unzipping experiment [16] in the entire range of f and T, whereas the phase diagram for a dsDNA of 16 base pairs differs significantly with the experiment. Since, under the periodic force, the chain may unzip and rezip, the bubble dynamics and the wandering interface (Y-fork junction) meeting transient bubbles (extra source of entropy) would play important roles in hysteresis. Needless to say such bubbles are ubiquitous in

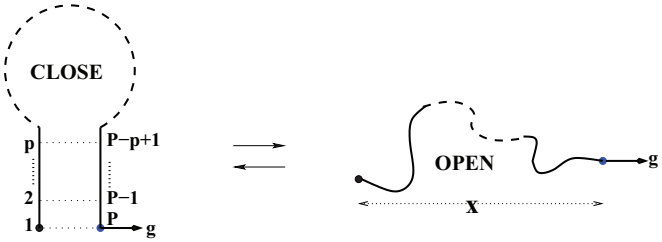

FIG. 1. (Color online) DNA hairpin in a zipped (Z) and an unzipped (U) state. The stem (solid lines) consists of complementary nucleotides, whereas the loop (dashed line) is made up of noncomplementary nucleotides. Only native interaction (dotted lines) for base pairing is allowed. For this paper, the stem is of length $p = 10$, and the loop has 12 monomers. The total length is $P = 32$.

a long chain. A DNA hairpin is the simplest model, where the premade loop allows us to study the dynamics of such implicit bubbles.

The outline of the paper is as follows. In Sec. II, we introduce the model used for the hairpin and the method of study. The results are analyzed in terms of average hysteresis loops and time-resolved loops. The dynamic phase diagram can be found in this section. In Sec. III, the hysteresis loops of an Ising ferromagnet under an asymmetric field modulation is given. The similarities with the DNA hairpin problem are discussed here. The paper ends with a short summary and conclusion in Sec. IV.

II. DNA HAIRPIN UNDER PERIODIC FORCE

A. Model and method

DNA hairpins (see Fig. 1) occur naturally *in vivo* and are used often in experiments on DNA with bubbles [28]. The nonpaired bases of the loop are a source of entropy which in turn controls the dynamics of hysteresis. In this paper, we perform Langevin dynamics (LD) simulations of a DNA hairpin [23] to study the separation x of the terminal base pairs pulled by a periodic force, $g(t)$, of time period $\tau(=1/\nu)$ (Fig. 2). There have been efforts [13,14] to understand transcriptionlike processes by applying a constant force in the middle of a DNA chain. A very rich phase diagram has been obtained though no such experiment has been reported so far to confirm the phase diagram. It appears that applying a force in the middle of the chain is experimentally difficult. Moreover, the biological situation requires the force following a moving replication fork, which is also not amenable to single-molecule force experiments. In view of these considerations, we use a simpler geometry where the force is applied at one end of the hairpin keeping the other end fixed, which could be used in single-molecule experiments. The typical time scale of fluctuations involved in unzipping varies from nanoseconds to microseconds, and therefore we avoid the details of an all atom simulation by adopting a minimal off-lattice coarse-grained model of a DNA hairpin, where each bead represents a nucleotide as a basic unit, which comprises a base, a sugar, and a phosphate group. We have performed our simulation in reduced units as discussed below.

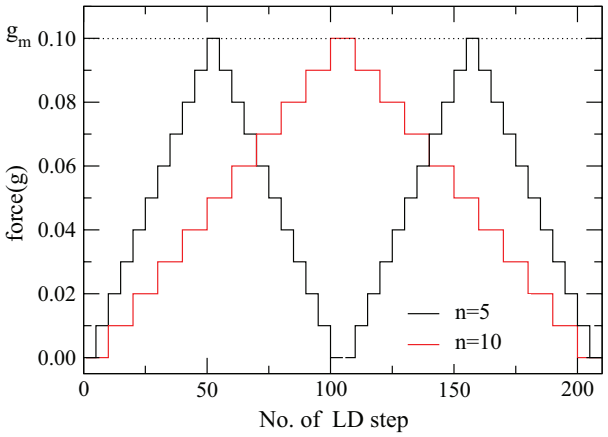

FIG. 2. (Color online) A typical periodic force used in the simulation. A cycle refers to one period of variation of the applied force g from 0 to g_m (called amplitude) and back to 0 at a fixed time period τ. This example has amplitude $g_m = 0.1$ and two different frequencies, $\nu = 1$ and $\tau = 0.38$ and 0.19 for $n = 5$ and 10, respectively.

1. Model

The configurational energy of the system under consideration is [23]

$$E = \sum_{i=1}^{P-1} k(d_{i,i+1} - d_0)^2 + \sum_{i=1}^{P-2} \sum_{j>i+1}^{P} 4\left(\frac{C}{d_{i,j}^{12}} - \frac{A_{ij}}{d_{i,j}^{6}}\right). \quad (1)$$

Here, $P = 32$ is the number of beads. The harmonic term with a spring constant, $k(=100)$, couples the adjacent beads along the chain. The distance between the adjacent beads $d_{i,j}$ is defined as $|\mathbf{r}_i - \mathbf{r}_j|$, where $\mathbf{r}_i$ and $\mathbf{r}_j$ denote the positions of beads i and j, respectively. We assign $C = 1$ of the Lennard-Jones (L-J) potential. The base pairing interaction $A_{ij} = 1$ is restricted to native contacts only, which is similar to the Go model. All pairs of nucleotides that do not form native contacts in the stem and in the loop interact only through short-range repulsion (excluded volume). The parameter $d_0(=1.12)$ corresponds to the equilibrium distance in the harmonic potential, which is close to the equilibrium position of the average L-J potential. We obtained the dynamics of the system by using the following Langevin equation [29,30],

$$m\frac{d^2\mathbf{r}}{dt^2} = -\zeta\frac{d\mathbf{r}}{dt} + \mathbf{F_c} + \Gamma, \quad (2)$$

where m is the mass of a bead which is set equal to 1 here, and the friction coefficient used in the simulation is $\zeta = 0.4$. $\mathbf{F_c}$ is defined as the gradient of the energy, $-\nabla E$, and Γ is a random force, a white noise with zero mean and correlation

$$\langle\Gamma_i(t)\Gamma_j(t')\rangle = 2\zeta k_B T\delta_{ij}(t - t'), \quad (3)$$

where k_B is the Boltzmann constant which is set to 1 in the present simulation. The choice of Eq. (3) keeps the temperature of the system constant throughout the simulation for a given force. In order to study the behavior of a DNA hairpin under a periodic force, we add an additional energy, $-g(t)x(t)$, to the total energy of the system in Eq. (1). We have performed the simulation at $T = 0.10$, for which $g_c \sim 0.20$ [31]. We may convert the dimensionless units to real units by using the

relations [29]

$$t^* = \left(\frac{m\sigma^2}{\epsilon}\right)^{1/2} t, \quad r^* = \sigma r, \tag{4}$$

where t^*, r^*, and ϵ are time, distance, and characteristic hydrogen bond energy in real units. Here σ is the distance at which the interparticle potential goes to zero. For example, if we set effective base pairing energy $\epsilon \sim 0.1$ eV, the average mass of each bead 5×10^{-22} g, and $\sigma = 5.17$ Å, we get a time unit $\tau \approx 3$ ps. It is known that ζ affects the kinetics only and the thermodynamics remains unchanged [32,33]. The friction coefficient used in our simulations is $\zeta = 0.4m\tau^{-1} = 6 \times 10^{-11}$ gs^{-1}. The order of force thus would be $\epsilon/\text{Å} \sim 160$ pN. For temperature conversion, a little more care is needed because the coarse-grained model does not take into account many other energies [34]. We compare the phase diagrams for DNA in the thermodynamic limit using a two-state model based on the modified freely jointed chain (mFJC) model of polymer with the experiment [16]. The melting temperature at 363 K and the flat portion (the stretching of covalent bonds) at 293 K in experiments [16] correspond to 0.23 and 0.05 in reduced units, which are also consistent with the simulation [23]. If we use this information to scale the temperature in a linear fashion, we have the relation $T^* = 363 + \frac{363-293}{0.23-0.05}(T - 0.23)$, where T^* is the real temperature. This mapping is valid only in the range of overlap of mFJC and experiment. This relation gives the reduced temperature used here, $T = 0.1$, as equivalent to a real temperature around 320 K, i.e., around 45 °C. It may be noted that hysteresis has been observed in this range of temperature [17].

2. *Integration*

The equation of motion is integrated using a sixth-order predictor corrector algorithm with the time step $\Delta t = 0.025$ [30]. Reference [23] showed that the present coarse-grained model exhibits the observed features of the experimental g-T diagram [16] of a long DNA with implicit bubbles as well as hysteresis at low temperatures in the g-x plane as seen experimentally [17]. During the simulation, g is changed in steps of $\Delta g(=0.01)$ from 0 to a maximum g_m and then to 0 (Fig. 2). This one period is referred to as *a cycle* and g_m as the amplitude. The time period

$$\tau = 2n\Delta t\left(1 + \frac{g_m}{\Delta g}\right)$$

is controlled by n, the number of LD steps executed after every increment (or decrement) of force. We choose n such that $n\Delta t$ is much below the equilibration time.

By changing g_m or ν, we find it is possible to induce a dynamical transition between a state of time-averaged zipped (Z) or unzipped (U) to a dynamical state (D) oscillating between Z and U.

B. Numerical analysis

1. *Hysteresis loops*

In Fig. 3, we plot the average value of $x(g)$ over $\mathcal{C}(=1000)$ cycles vs g, for different values of g_m and ν. These loops for different initial conformations remain almost the same [except

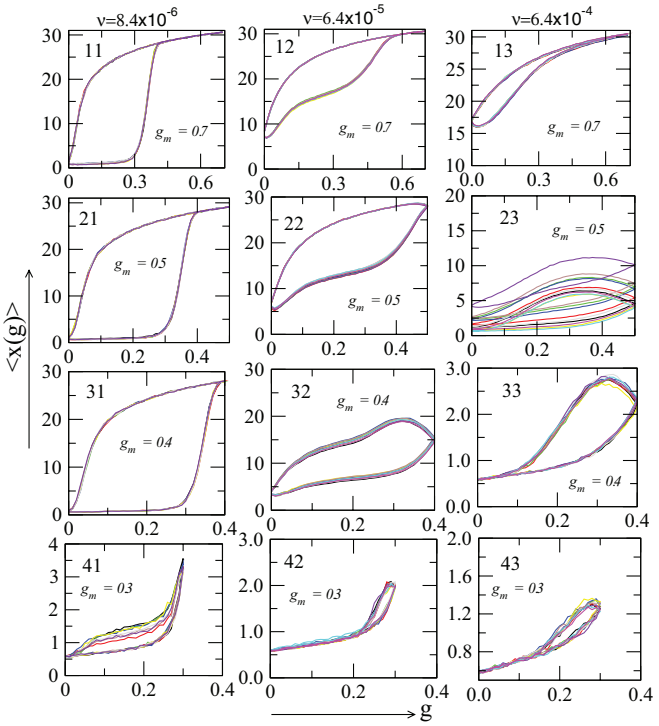

FIG. 3. (Color online) DNA hysteresis for different g_m and ν (increases from left to right) as indicated. Each plot contains the loops for ten different initial conformations. These are at $T = 0.10$, for which $g_c \sim 0.20$.

Fig. 3(23)] so that the large menagerie of shapes of hysteresis loops observed are typical, not exceptional or accidental. At a high frequency, the DNA remains in Z or in U depending on whether $g_m < 2g_c$ or not, [Figs. 3(13) and 3(43)], irrespective of the initial conformation. For a relatively smaller ν, the sequence of hysteresis loops [Figs. 3(11), 3(21), and 3(31)] is of a different nature. These clearly reflect that the DNA starts from the Z ($x = 0$ at the start of the cycle), goes to the U ($x = 30$), and then back to the Z [35]. Some of these plots show the phase lag between the force and the extension; e.g., even when the applied force decreases from g_m to 0 [Figs. 3(32) and 3(33)], the extension $x(g)$ increases. If the system gets enough time to approach equilibrium, the lag disappears [e.g., Figs. 3(21) and 3(31)]. A different behavior is seen in the case of intermediate forces [Figs. 3(21), 3(22), and 3(23)]. Despite the identification of the states at the two extreme forces as Z and U, there is a significant change in the x values at $g = 0$ and $g = g_m$, in Fig. 3(23), compared to the other loops shown in Fig. 3. Most striking here is the wide sample to sample fluctuations in the loop.

2. *Time-resolved loops*

The failure of the average response to provide a description of the steady-state dynamic behavior prompts us to analyze the distribution of paths over the different cycles in terms of a dynamical order parameter Q defined as

$$Q = \frac{1}{\tau}\int_0^\tau x(t)\,dt. \tag{5}$$

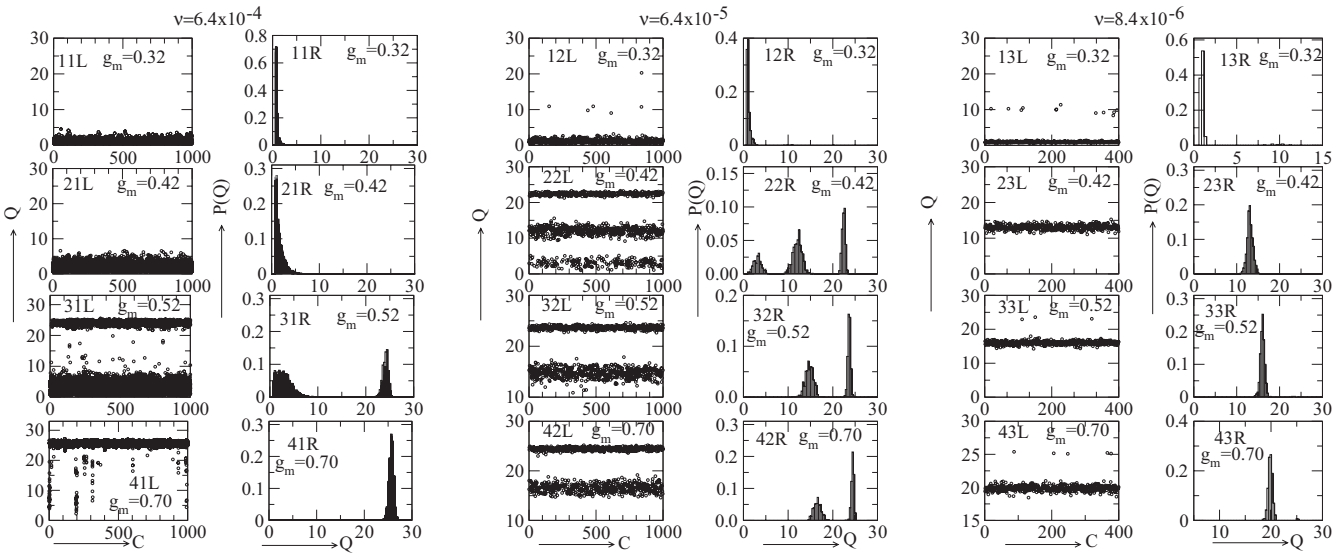

FIG. 4. The time sequence of Q and $P(Q)$ vs Q plots. Three pairs of vertical panels for three ν's. Each panel has (i) the time sequence on the left (L) and (ii) the $P(Q)$ plot on the right (R) for different g_m's.

This Q is analogous to the dynamical order parameter studied in the context of magnetic systems [26]. In Fig. 4, we plot the values of Q over different cycles for three different ν. The time sequence of Q seems not to indicate any regular pattern, and therefore, we assume that the allowed states occur randomly. The time sequence can then be interpreted in terms of a probability of getting a particular value of Q. We find that the steady state is described by a stationary probability distribution, $P(Q)$, which are also shown in Fig. 4. The plots show three peaks which could be associated with phases U, D, and Z by comparing with Fig. 3. Based on the width of $P(Q)$ we make operational criteria, $0 < Q_Z < 10$, $Q_U > 22$, and $10 < Q_D < 22$, for the identification of the phases.

From the peak locations of $P(Q)$, we map out the phase diagram of the driven DNA in the g-ν plane (Fig. 5). A line in Fig. 5 represents a boundary beyond which a particular peak appears or disappears and resembles a first-order line. These are now discussed sequentially.

(1) For a very small force, $P(Q)$ expectedly shows a peak in the Q_Z window for any ν (Fig. 4, first row). Beyond a certain g_m there appears a second peak in the Q_D window. See Figs. 4(12) to 4(22) or Figs. 4(13) to 4(23). For each chosen ν, we determined the value of g_m above which the peak of Q_D appears, giving us the lower boundary for D.

(2) For a given ν, with increasing g_m, the peak height of Q_Z decreases as seen in Fig. 4 along any vertical sequence, top to bottom. One gets one or two other peaks but Z disappears beyond a certain g_m, giving an upper boundary for Z.

(3) Before Z disappears, there could be peaks for D or U, or both [Figs. 4(31) and 4(22)], implying coexistence, Z + U or Z + D + U, for a range of g_m. From the appearance of U, we determine the lower boundary for U.

(4) Then, as Z disappears, the system may be either in the D phase [Fig. 4(23R)] or in the mixed state of D + U [Fig. 4(32R)]. To be noted is the crossing of the boundaries of U and Z, which produces the region of the D phase. Once the mixed phase D + U appears, a further increase of g_m vanishes the D peak and only the U peak survives.

An important point is the occurrence of different Q values or regions of phase coexistence. In such a situation, the average response is not a good measure of the state and there will be intrinsic difficulty in reducing fluctuations in the hysteresis curve.

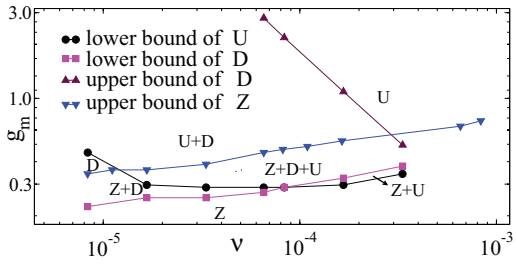

FIG. 5. (Color online) Dynamical phase diagram of a periodically driven DNA hairpin in the g_m-ν plane. The lines are boundaries for various phases: U, D, and Z. The points are from the simulation and the lines are guides to the eye.

III. DYNAMICAL PHASE TRANSITION IN ISING FERROMAGNET

To use the magnetic analogy, consider a ferromagnet like a two-dimensional Ising model below its critical point, subjected to a periodic magnetic field $h = h_0 \cos(2\pi\nu t)$ in time (t). As ν increases, there is a dynamic transition where the average magnetization in a cycle goes from zero to a nonzero value [26]. For small ν there is a hysteresis loop connecting the two symmetrically opposite magnetized states, while for large ν the lethargic system remains magnetized in one direction. The analogy is between the conjugate pair (h,m), where m is the magnetization, for a magnet and (g,x) for DNA. The magnetic hysteresis loop in the h-m plane is analogous to that in the g-x plane. To simulate a DNA-like behavior in the Ising system, an

asymmetric modulation of the magnetic field has been taken to make the average field over a cycle different from the critical value. A Monte Carlo dynamics is used to study the hysteresis in an 8×8 square lattice Ising model with periodic boundary conditions under a periodic field between h_l and h_m.

A. Model and method

We consider a two-dimensional Ising spin system ($\{s_i = \pm 1\}$) with nearest-neighbor interaction and under a magnetic field h,

$$H = -J \sum_{\langle i,j \rangle} s_i s_j - h \sum_i s_i, \qquad (J > 0), \tag{6}$$

with i labeling the sites of an 8×8 square lattice with periodic boundary conditions. The infinite lattice critical temperature is $T_c \approx 2.269 J/k_B$ in zero field. The magnetization is defined as the thermal average,

$$m = N^{-1} \sum_i \langle s_i \rangle, \tag{7}$$

of $N(=64)$ spins. For the above Hamiltonian, we choose $J = 1$ and $k_B T = 2$, with $k_B = 1$, so that $T < T_c$.

The Monte Carlo (MC) procedure used is as follows. We choose a spin and calculate the change in energy ΔE of the system if the spin gets flipped. Whether this spin would be flipped or not is determined by using the standard Metropolis algorithm, which gives the probability of acceptance of an attempted flip by $P_{\text{accept}} = \min(1, e^{-\beta \Delta E})$. In this way, we sequentially consider all the N spins, one at a time, to attempt a flip. The time taken to attempt N spin flips constitutes one MC sweep.

A complete cycle consists of $2\mathcal{N}$ steps, starting from h_l, reaching h_m and then back to h_l. Initially the system is equilibrated at $h_l = -0.6$ and $k_B T = 2$. Then the periodic magnetic field is switched on. At each step, (i) the magnetic field is increased by $\delta h = (h_m - h_l)/\mathcal{N}$ and (ii) the system is relaxed towards equilibrium by $n = 5$ MC sweeps, which is much less than the equilibration time. The magnetization m is calculated at each of such $2\mathcal{N}$ steps. The average of magnetizations calculated over a cycle then gives the quantity Q. The above process is repeated $\mathcal{C} = 10^4$ times, i.e., for 10^4 cycles. The Q values obtained in this way give the probability distribution $P(Q)$ for a given h_m. We simulate the system for various frequencies (controlling $\mathcal{N}$) and h_m, keeping h_l fixed.

An asymmetric field in the Ising model enables us to distinguish two differently ordered phases, the counterparts of the zipped and the unzipped states, and in addition a *hysteretic state*, to be called the *dynamic state* D. For easy comparison, the negatively magnetized state is named Z while the positively magnetized state is U. The states are distinguished by a dynamic parameter,

$$Q = \frac{1}{\tau} \int_0^\tau m(t)\, dt, \tag{8}$$

and the operational definition adopted is (i) $Q_{\text{Z}} \equiv \{-64 \leqslant Q \leqslant -40\}$, (ii) $Q_{\text{U}} \equiv \{55 \leqslant Q \leqslant 64\}$, and (iii) the rest is Q_{D}. Cases (i) and (ii) occur when the paths in the m-h diagram remain on one side throughout the cycle, and case (iii), the dynamical state D, occurs either if there are paths connecting positive and negative values of magnetization or if the paths remain more or less near zero of magnetization. The division of the three intervals or regions are independent of h_m.

B. Numerical results

The results for $P(Q)$ vs Q shown in Fig. 6 are very similar to those shown in Fig. 4 and the interpretations toe the DNA line. We point out a few salient features here. For $h_m \leqslant 0$, there is only the Z state [Figs. 6(a)–6(c)]. With increasing h_m, $P(Q)$ develops a multipeaked structure which indicates coexistence. Various sequences of states seen are noted in the figure caption. These include D + U, Z + D, and Z + D + U. We find a clear dependence on ν of the occurrence of the various states, similar to the DNA case. There are situations where U appears before Z vanishes. In this regime, we see the coexistence of three phases, Z + D + U (e.g., $h_m = 0.6$ in Fig. 6). The peak height for D first grows from zero and then, depending on frequency, it may decrease, with the gradual appearance of a U peak [Figs. 6(a) and 6(b)], or it may keep on increasing up to a very high field seemingly merging with U [low frequency case of Fig. 6(c)]. The Ising case has a special line at $h_m = -h_l$ where the $+ \leftrightarrow -$ symmetry is restored. On that line, there is the dynamic transition (D $\leftrightarrow$ Z or U) at a particular frequency [26]. The occurrence of the Z + D + U coexistence region found on this line is a finite size effect and is a novelty of the mesoscopic system. The h-ν phase diagram is qualitatively similar to that of the DNA hairpin, shown in Fig. 5.

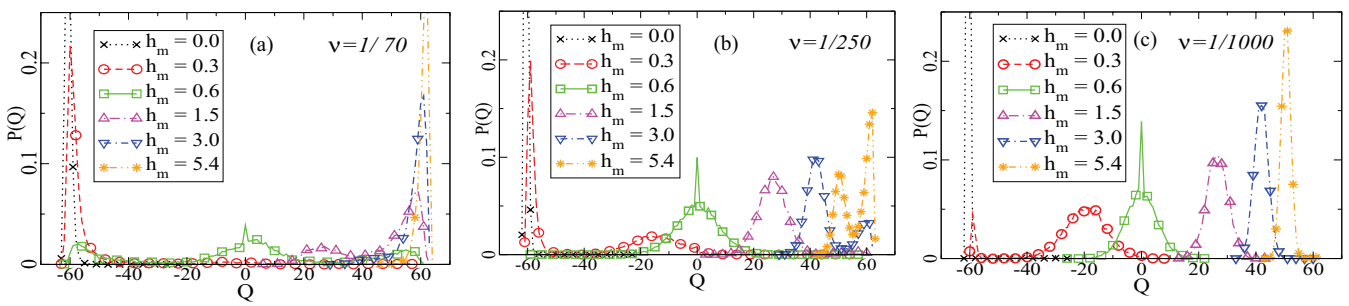

FIG. 6. (Color online) $P(Q)$ vs Q for the Ising model for three different ν's and the same set of h_m with $h_l = -0.6$. For a given ν, the distribution $P(Q)$ shifts as h_m increases. It goes from Z to U through D. The sequence of phases are (a) Z $\rightarrow$ Z + D $\rightarrow$ Z + D + U $\rightarrow$ D + U $\rightarrow$ U, (b) Z $\rightarrow$ Z + D $\rightarrow$ D $\rightarrow$ D + U, and (c) Z $\rightarrow$ Z + D $\rightarrow$ D.

IV. SUMMARY

This paper reports the possibility of a dynamical transition of a DNA hairpin and a magnetic spin system both under a periodic drive. When a DNA hairpin is subjected to a periodic force or a magnetic system is subjected to a periodic magnetic field, then the system driven away from equilibrium shows hysteresis. Usually to get the hysteresis curve, one averages over many cycles of the field or force, but we show here that this averaging suppresses or loses the actual picture of the states. This can be observed if one looks at the individual cycles. By quantifying the state of a cycle by Q, the average separation for DNA, or the average magnetization for the spins, we find that the distribution of Q is multipeaked. Whenever a distribution is multipeaked, the average is not a good representation of the state. We identify the peaks of the distribution with the zipped (Z), unzipped (U), and dynamical (D) states for the DNA hairpin. There is a dynamical transition from one phase or state to another phase, and also there is coexistence of phases in some range of strength of drive and frequency. The phase diagrams constructed from the data for both the DNA hairpin and the magnetic system are of a similar nature. The role of hysteresis in biological processes remains unexplored territory. On a more quantitative front, our work calls for time-resolved experiments on periodically driven DNA hairpins to explore such hitherto unknown dynamical phase diagrams.

ACKNOWLEDGMENTS

G.M. and S.K. would like to thank CSIR and DST, India, for financial support. We thank IUAC, New Delhi for the generous computer support.

[1] J. D. Watson *et al.*, *Molecular Biology of the Gene*, 5th ed. (Cold Spring Harbor Laboratory Press, Cold Spring Harbor, NY, 2003).
[2] S. M. Bhattacharjee, J. Phys. A **33**, L423 (2000), arXiv:cond-mat/9912297.
[3] T. R. Strick, J.-F. Allemand, D. Bensimon, A. Bensimon, and V. Croquette, Science **271**, 1835 (1996).
[4] U. Bockelmann, B. Essevaz-Roulet, and F. Heslot, Proc. Natl. Acad. Sci. USA **94**, 11935 (1997).
[5] S. M. Bhattacharjee and F. Seno, J. Phys. A **36**, L181 (2003); S. M. Bhattacharjee, Europhys. Lett. **65**, 574 (2004); J. Phys.: Condens. Matter **22**, 155102 (2010); M. D. Betterton and F. Jülicher, *ibid.* **17**, S3851 (2005).
[6] K. L. Sebastian, Phys. Rev. E **62**, 1128 (2000).
[7] D. K. Lubensky and D. R. Nelson, Phys. Rev. Lett. **85**, 1572 (2000).
[8] D. Marenduzzo, A. Trovato, and A. Maritan, Phys. Rev. E **64**, 031901 (2001).
[9] S. Kumar, I. Jensen, J. L. Jacobsen, and A. J. Guttmann, Phys. Rev. Lett. **98**, 128101 (2007).
[10] Y. Kafri, D. Mukamel, and L. Peliti, Eur. Phys. J. B **27**, 135 (2002).
[11] S. Kumar and G. Mishra, Phys. Rev. E **78**, 011907 (2008).
[12] P. Sadhukhan, J. Maji, and S. M. Bhattacharjee, Europhys. Lett. **95**, 48009 (2011).
[13] R. Kapri, S. M. Bhattacharjee, and F. Seno, Phys. Rev. Lett. **93**, 248102 (2004).
[14] D. Giri and S. Kumar, Phys. Rev. E **73**, 050903(R) (2006).
[15] R. Kapri, J. Chem. Phys. **130**, 145105 (2009).
[16] C. Danilowicz, Y. Kafri, R. S. Conroy, V. W. Coljee, J. Weeks, and M. Prentiss, Phys. Rev. Lett. **93**, 078101 (2004).
[17] K. Hatch, C. Danilowicz, V. Coljee, and M. Prentiss, Phys. Rev. E **75**, 051908 (2007).
[18] S. Kumar and M. S. Li, Phys. Rep. **486**, 1 (2010).
[19] R. Bundschuh and U. Gerland, Eur. Phys. J. E **19**, 347 (2006).
[20] I. Donmez and S. S. Patel, Nucl. Acids Res. **34**, 4216 (2006).
[21] S. S. Velankar, P. Soultanas, M. S. Dillingham, H. S. Subramanya, and D. B. Wigley, Cell **97**, 75 (1999).
[22] M. F. Williams and E. Jankowsky, J. Mol. Biol. **415**, 819 (2012).
[23] G. Mishra, D. Giri, M. S. Li, and S. Kumar, J. Chem. Phys. **135**, 035102 (2011).
[24] R. Kapri, Phys. Rev. E **86**, 041906 (2012).
[25] G. Bertotti, *Hysteresis in Magnetism: For Physicists, Material Scientists, and Engineers* (Academic Press, San Diego, 1998).
[26] B. K. Chakrabarti and M. Acharyya, Rev. Mod. Phys. **71**, 847 (1999).
[27] A. N. Gupta *et al.*, Nat. Phys. **7**, 631 (2011).
[28] G. Bonnet, O. Krichevsky, and A. Libchaber, Proc. Natl. Acad. Sci. USA **95**, 8602 (1998); S. Kumar, D. Giri, and Y. Singh, Europhys. Lett. **70**, 15 (2005).
[29] M. P. Allen and D. J. Tildesley, *Computer Simulations of Liquids* (Oxford Science, Oxford, UK, 1987).
[30] D. Frenkel and B. Smith, *Understanding Molecular Simulation* (Academic Press, London, 2002).
[31] The value $g_c \sim 0.2$ is from Fig. 4(a) of Ref. [23], marked by an arrow there. We have chosen $T = 0.1$ because hysteresis starts occurring as noted there.
[32] C. Hyeon and D. Thirumalai, Proc. Natl. Acad. Sci. USA **102**, 6789 (2005).
[33] M. S. Li, M. Kouza and C-K. Huym, Biophys. J. **92**, 547 (2007).
[34] This estimate of ϵ is not sufficient for temperature conversion. For example, we may get the melting temperature right for the finite chain of 32 nucleotides, ≈317 K, which corresponds to $T_m = 0.21$ in reduced units as reported in Ref. [23] and is consistent with the one obtained by OligoCalc (W. A. Kibbe, Nucl. Acids Res. **35**, W43 (2007) for the same sequence. However, this conversion leads to a force-induced melting temperature of 158 K at force 32 pN [32,33], which corresponds to temperature 0.1 and force 0.2, respectively, in reduced units. This low temperature looks consistent with the low estimate of $T = 250$ K found in Ref. [32] at force 15 pN.
[35] If $\langle x \rangle$ is less than 5, the system is in the zipped state and above than 5 it is in the unzipped state. This choice is consistent with the specific heat vs. T curve shown in Figs. 3(a) and 5 of Ref. [23].